ACS OMEGA

Open Access
This article is licensed under CC-BY-NC-ND 4.0

http://pubs.acs.org/journal/acsodf
Article

# Enhancement of Thermal, Mechanical, and Oxidative Properties of Polypropylene Composites with Exfoliated Hexagonal Boron Nitride Nanosheets

Amit Kumar Sonker,[#] Man Hieu Tran,[#] Nathan Park, Gouri Sankar Das, Hansa Mahajan, Tae Hee Lee,* and TaeYoung Kim*

**Cite This:** *ACS Omega* 2025, 10, 1853−1861

**Read Online**

ACCESS | Metrics & More | Article Recommendations | Supporting Information

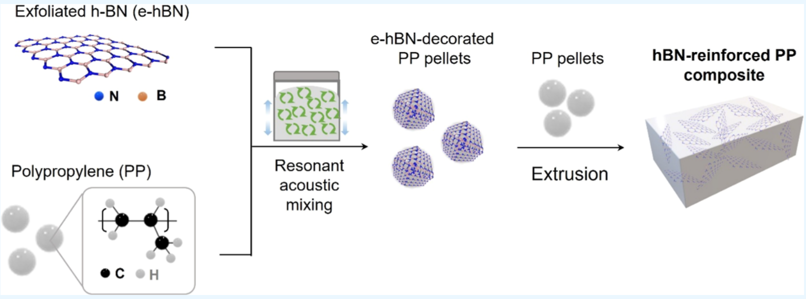

**ABSTRACT:** This study investigates the enhancement of polypropylene (PP) composites through the incorporation of exfoliated hexagonal boron nitride (h-BN) nanosheets. The preparation process involved exfoliating h-BN in a liquid phase using a high-pressure homogenizer, followed by the coating of PP pellets with the exfoliated nanosheets using an acoustic mixer. Melt extrusion was then employed to fabricate h-BN-reinforced PP composite films. Characterization techniques, including scanning electron microscopy, confirmed the uniform dispersion of exfoliated h-BN within the PP matrix, which is crucial for improving thermal conductivity, mechanical strength, and oxidative stability. Tensile testing demonstrated that exfoliated h-BN significantly enhanced the strength and toughness of homopolymer PP, while the improvements in impact copolymer PP were more modest. Thermal analysis revealed no significant change in the decomposition temperatures of PP but indicated improved oxidative stability with the incorporation of h-BN nanosheets. Notably, the oxidation resistance of PP was enhanced, as evidenced by reduced carbonyl index values in thermally aged samples. Overall, exfoliated h-BN nanosheets significantly improve the performance of PP composites, demonstrating their potential for diverse industrial applications that require superior thermal and mechanical properties, as well as enhanced oxidation resistance.

## 1. INTRODUCTION

Polypropylene (PP) is a widely used thermoplastic in various industrial sectors due to its excellent mechanical properties, low cost, outstanding electrical insulation, and ease of processing. These attributes make PP a versatile material, commonly applied in automotive, packaging, electrical and electronic devices, and biomedical industries.[1] Notably, PP has also emerged as a potential alternative to cross-linked polyethylene (XLPE) for use as an electrical insulation material in power cables.

Despite these advantages, PP has inherent limitations that restrict its performance in high-demand applications. These include poor thermal conductivity, low oxidation resistance, and limited mechanical strength under specific conditions. Additionally, PP has a relatively low melting point and is susceptible to thermal degradation when exposed to elevated temperatures for prolonged periods. This degradation, driven by oxidative processes, produces carbonyl and hydroperoxide groups, leading to molecular chain scission, cross-linking, and the formation of volatile degradation products. These effects deteriorate the mechanical and physical properties of the polymer, particularly in high-temperature applications.

To overcome these limitations, there has been a growing interest in enhancing PP's properties through the incorporation of various fillers, particularly nanoscale materials.[2−4] Numerous studies have investigated the reinforcement of PP with nanomaterials such as carbon nanotubes, graphene, and nanoclays, aiming to improve its thermal, mechanical, and oxidative properties.[5−10] These efforts focus on improving the

**Received:** November 24, 2024
**Revised:** December 23, 2024
**Accepted:** December 30, 2024
**Published:** January 6, 2025

© 2025 The Authors. Published by American Chemical Society

thermal stability, oxidative resistance, mechanical strength, and stiffness of PP, expanding its applicability to more demanding operational conditions.[11−15]

Among the various fillers explored, hexagonal boron nitride (h-BN) has gained significant attention as a promising candidate.[16] h-BN is known for its unique combination of high thermal conductivity, excellent electrical insulation, chemical inertness, and robust mechanical properties.[17−21] Structurally, h-BN consists of a two-dimensional crystalline framework of alternating boron and nitrogen atoms, similar to graphite. This configuration provides exceptional thermal conductivity (up to 600 W/m·K) and stability at temperatures exceeding 1000 °C.[22−24] Furthermore, h-BN exhibits low thermal expansion, high hardness, and intrinsic lubricating properties, making it an ideal reinforcement material for polymer matrices.[25−27]

Incorporating h-BN into a PP matrix offers several benefits, primarily stemming from its unique structural and functional properties. Its two-dimensional platelet morphology allows for uniform dispersion within the polymer matrix, facilitating strong interfacial adhesion and efficient heat transfer. This results in enhanced thermal conductivity and stability, making the composite well-suited for applications requiring effective thermal management, such as electrical insulation in power cables.[25−27]

h-BN's ability to mitigate thermal oxidation further enhances the composite's resistance to elevated temperatures, helping maintain its mechanical and physical properties over time. In addition to its thermal advantages, h-BN's excellent electrical insulation properties make it especially beneficial for PP composites in environments where minimizing electrical conductivity is crucial to prevent short circuits and electrical failures. The combined thermal conductivity and electrical insulation offered by h-BN is a rare and valuable attribute among filler materials, presenting a multifunctional solution for polymer composites. Beyond improving thermal and electrical properties, the inclusion of h-BN also significantly enhances the mechanical performance of PP. Reinforced composites exhibit increased tensile strength, enhanced modulus, and improved impact resistance, making them ideal for structural applications that require materials capable of withstanding diverse mechanical stresses.

Despite these advantages, one major challenge in previous studies is the poor dispersion of h-BN in the polymer matrix, which limits the effectiveness of the filler. Exfoliating h-BN into nanosheets has been shown to improve its dispersion and, subsequently, the overall performance of the composite. Methods such as high-pressure homogenization and microfluidization have been explored to achieve exfoliation, but these processes are often not fully optimized in the context of PP composites. While h-BN has been incorporated into PP in several studies, the specific role of exfoliation and its effect on the performance of PP composites have not been systematically examined. Many studies focus on the bulk properties of composites without addressing the crucial influence of exfoliation and dispersion, which significantly impact the thermal, mechanical, and oxidative properties of the final material. Furthermore, there is limited understanding of how exfoliated h-BN nanosheets influence the dispersion in the PP matrix and how they affect the long-term stability and performance of PP composites under thermal aging.

This study aims to fill this gap by focusing on the exfoliation of h-BN using a high-pressure homogenizer and examining its impact on the mechanical, thermal, and oxidative properties of PP composites. The novelty of this research lies in using exfoliated h-BN nanosheets to enhance the performance of PP composites, with an emphasis on improving their dispersion within the PP matrix. It is hypothesized that better dispersion of exfoliated h-BN will lead to superior mechanical reinforcement, enhanced thermal conductivity, and improved oxidative stability of the PP composite materials.

Additionally, this study provides a comprehensive evaluation of the effects of exfoliated h-BN on thermal degradation, oxidative stability (measured via Oxidative Induction Time, OIT), and long-term performance of PP composites under thermal aging conditions, which has not been adequately explored in previous studies.

## 2. MATERIALS AND METHODS

**2.1. Materials.** Hexagonal boron nitride (h-BN) was procured from Denka, Japan. Poly(4-vinylpyridine) (P4VP) with a molecular weight of approximately 60,000 was sourced from Sigma-Aldrich. *N*-methyl-2-pyrrolidone (NMP) was obtained from Daejung Chemicals (South Korea). Two types of polypropylene (PP), homopolymer (HP) and impact copolymer (IP), were supplied by LyondellBasell, Netherlands.

**2.2. Exfoliation of h-BN.** For the exfoliation of h-BN, 0.5 vol % of h-BN was dispersed in 100 mL of NMP, to which 0.25 vol % of P4VP was added as a dispersing agent. This mixture was homogenized using a Silverson mixer (LSM) operating at 5000 rpm for 1 h. Subsequently, it was processed through an M110P microfluidizer (Microfluidics Corp.) equipped with a Z-type interaction chamber containing ∼87 μm wide microchannels. The system operated at 190 MPa for 5 cycles, with each cycle defined as a single pass through the rotor chamber. The exfoliated h-BN (referred to as e-hBN) was collected by centrifugation, followed by washing and freeze-drying to remove residual NMP.

**2.3. Preparation of h-BN-Reinforced PP Composite.** Prior to melt extrusion, the h-BN and e-hBN powders were mixed with PP pellets using a Resodyn LabRAM II acoustic mixture. Composite samples were fabricated using a Thermo scientific melt extruder (process 11 parallel-twin Hake extruder) and subsequently molded into sheets with a Carver compression molding machine. Neat PP sheets were prepared by hot-pressing PP pellets directly using the compression molding machine at a pressure of six metric tons.

**2.4. Characterization.** X-ray diffraction (XRD) measurements were conducted using a Rigaku instrument (model no. RINT-2000) with Cu K$\alpha$ radiation to confirm the exfoliation of h-BN nanosheets. Scans were conducted in the 2$\theta$ range of 5−80° at a rate of 1°/min. 3D X-ray microscope (XRM) images were obtained using a ZEISS, Xradia 520 Versa microscope to analyze the dispersion of h-BN within the PP matrix. Scanning electron microscopy (SEM) analysis was conducted using a JEOL JSM-7500F microscope to observe h-BN nanosheets and their dispersion. Differential scanning calorimetry (DSC) measurements were performed using a PerkinElmer Q4000 instrument to determine oxidation induction time (OIT) in accordance with ASTM D3895-14.[28] Samples were heated from 30 to 180 °C at a rate of 10 °C/min under a nitrogen atmosphere. Once the temperature reached 180 °C, the samples were held isothermally for 1 min before being exposed to an oxygen atmosphere. During this isothermal phase, heat flow was recorded as a function of time to evaluate thermal oxidation behavior and stability. Heat

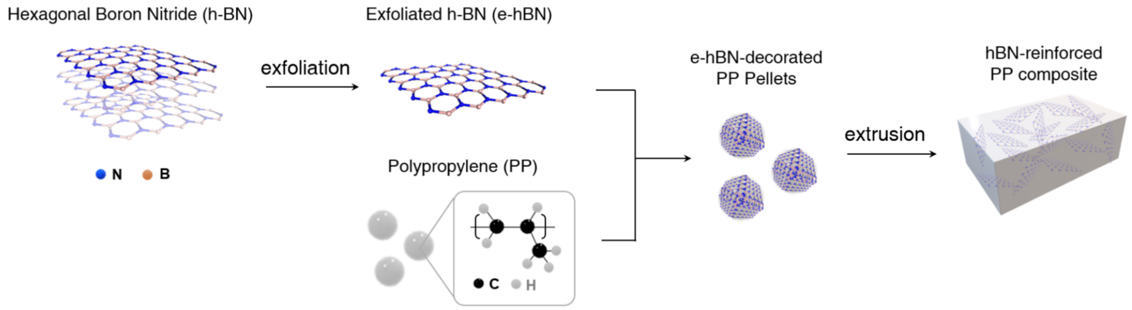

**Figure 1.** Schematic representation of the procedure for preparing h-BN-reinforced PP composites.

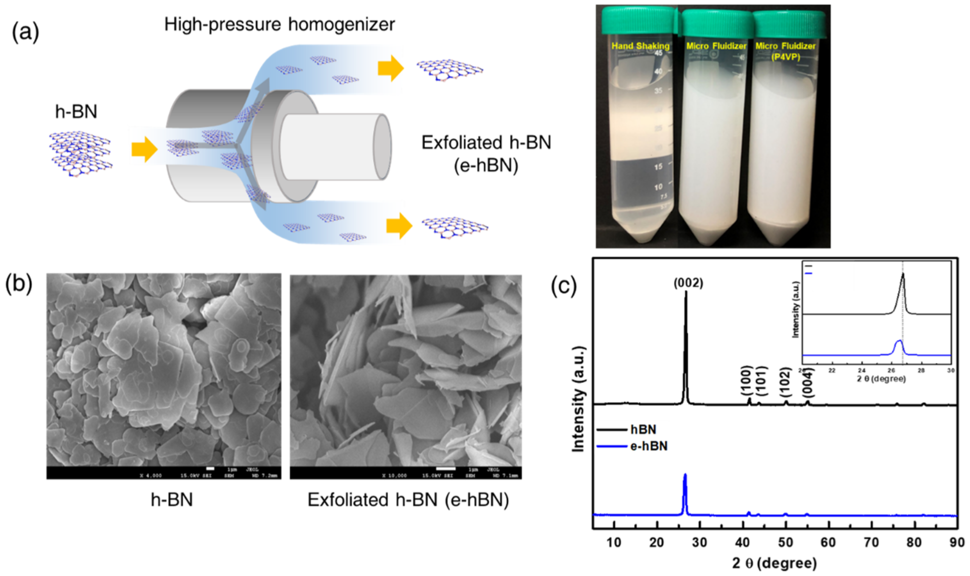

**Figure 2.** (a) Liquid-phase exfoliation of h-BN using a high-pressure homogenizer. Inset: photograph of exfoliated h-BN dispersion. (b) SEM images of bulk and exfoliated h-BN. (c) XRD patterns of bulk and exfoliated h-BN.

capacity measurements followed ASTM E1269-11. Thermal conductivity was calculated using the equation $k = \alpha \cdot \rho \cdot c$, where $\alpha$, $\rho$, and $c$ are thermal diffusivity, density, and heat capacity, respectively. Thermal diffusivity was measured using MTPS method (Trident, Canada) and density was determined using a density tester (MH-300A, Qunlong, China). Thermogravimetric analysis (TGA) was conducted using a TA Instruments SDT Q600 to assess thermal stability. Samples were scanned from 30 to 800 °C at a heating rate of 10 °C/min under nitrogen. Tensile tests were performed using a Zwick Roell universal testing machine (UTM) following ASTM D882-12. Specimen measured 6 cm × 3 cm × 0.3 cm with a 4 cm gauge length. Fourier transforms infrared spectroscopy (FTIR) spectra were recorded using a Thermo Scientific Nicolet 6700 FTIR Spectrometer. Samples were thermally aged in a JEIO TECH model OF-2GW oven at 120 °C for 250 and 500 h. Postaging, FTIR was used to determine the carbonyl index (ratio of the carbonyl peak at 1700−1800 $\text{cm}^{-1}$ to the reference peak at 2720 $\text{cm}^{-1}$) as an indicator of thermal degradation.[12]

## 3. RESULTS AND DISCUSSION

**3.1. Characterization of hBN-Reinforced PP Composites.** The fabrication of h-BN-reinforced polypropylene (PP) composites followed a systematic methodology designed to achieve uniform dispersion of the exfoliated nanofillers within the polymer matrix, as outlined in Figure 1. The process involved the exfoliation of h-BN powders in the liquid phase, followed by coating the exfoliated nanosheets onto PP pellets using an acoustic mixer. These coated pellets were subsequently fed into a melt extruder to produce h-BN-reinforced PP composite films.

To ensure effective exfoliation and uniform dispersion of h-BN nanosheets, a liquid-phase exfoliation process utilizing a high-pressure homogenizer was employed (Figure 2a). This method relies on the application of intense shear forces and high pressure, which effectively overcome the strong van der Waals forces between the layers of bulk h-BN. The h-BN suspension is forced through a narrow gap at high velocities, generating extreme turbulence and shear stress necessary to separate the thick layers into thin nanosheets. The resultant exfoliated nanosheets displayed a stable whitish suspension, visually confirming successful exfoliation.

The exfoliation process was further validated using scanning electron microscopy (SEM), as shown in Figure 2b. The images reveal that bulk h-BN comprises thick, stacked layers, whereas exfoliated h-BN nanosheets exhibit significantly reduced thickness and increased lateral dimensions. This morphological transformation enhances the surface area of the h-BN nanosheets, promoting better interfacial interaction with the PP matrix and contributing to the improved properties of the composite. X-ray diffraction (XRD) analysis provided additional evidence of successful exfoliation (Figure 2c). The XRD patterns of bulk h-BN showed characteristic diffraction

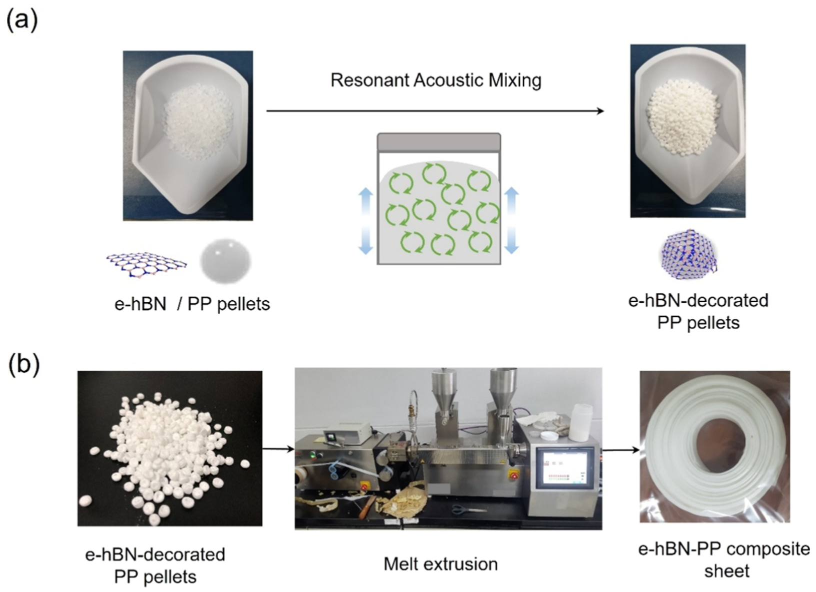

**Figure 3.** Preparation of e-hBN-reinforced PP composite. (a) Coating PP pellets with e-hBN nanosheets using resonant acoustic mixer, (b) Melt extrusion of e-hBN-coated PP pellets into composite sheets.

peaks at $2\theta$ values of 26.8, 41.7, 43.9, 50.2, and 55.2°, corresponding to the (002), (100), (101), (102), and (004) planes of hexagonal-phase h-BN, respectively[29,30] a significant reduction in the intensity of the (002) peak was observed, accompanied by peak broadening. These changes indicate a weakening of layer stacking along the C-axis, confirming the separation of h-BN layers.[31] Furthermore, the shift of the (002) peak to 26.3° with an interspacing ($d_{002}$) of 0.35 nm is indicative of increased interlayer separation, validating the successful production of exfoliated h-BN nanosheets.[32]

The preparation of polypropylene (PP) composites reinforced with exfoliated h-BN (e-hBN) nanosheets involved two key steps, as illustrated in Figure 3. In the first step, the e-hBN nanosheets were uniformly coated onto PP pellets using a resonant acoustic mixer (Figure 3a). The high-frequency sound waves generated by the acoustic mixer create rapid vibrations, enabling uniform dispersion and effective adhesion of e-hBN nanosheets onto the PP pellet surfaces. This step is critical as it ensures that the nanosheets are evenly distributed within the polymer matrix during subsequent processing, enhancing the composite's overall homogeneity and performance. In the second step, the h-BN-coated PP pellets were subjected to a melt extrusion process (Figure 3b). During this process, the mixture was heated to melt the PP, facilitating thorough blending of the nanosheets with the polymer matrix. This approach not only ensures the uniform incorporation of e-hBN but also promotes strong interfacial bonding between the filler and the polymer.

Two types of PP, homopolymer (HP) and impact copolymer (IP), were used in this study to explore the influence of polymer structure on the composite properties. HP consists entirely of propylene monomers, characterized by higher crystallinity and stiffness. Conversely, IP contains both propylene and ethylene monomers, where the ethylene is distributed as rubbery domains within the propylene matrix. The rubbery domains in IP enhance toughness and impact resistance, making it suitable for applications requiring superior mechanical shock absorption and low-temperature performance.

To streamline the discussion of results, the nomenclature of the various PP composites is summarized in Table 1. Both HP and IP matrices were reinforced with either stacked h-BN or exfoliated e-hBN at a filler content of 5 wt %.

**Table 1. Nomenclature of PP and h-BN-Reinforced PP Composites**

| samples | h-BN (wt %) | PP (wt %) | remark |
|---|---|---|---|
| HP | 0 | 100 | PP homopolymer |
| IP | 0 | 100 | Impact PP, PP copolymer |
| hBN-HP | 5 | 95 | Stacked hBN |
| hBN-IP | 5 | 95 | Stacked hBN |
| e-hBN-HP | 5 | 95 | exfoliated hBN (e-hBN) |
| e-hBN-IP | 5 | 95 | exfoliated hBN (e-hBN) |

The mechanical and thermal properties of the prepared composites were comprehensively evaluated to assess the effects of e-hBN reinforcement and the influence of polymer matrix type. By systematically comparing samples containing stacked h-BN and e-hBN within the HP and IP matrices, the study highlights the superior performance of e-hBN-based composites in terms of thermal stability, mechanical strength, and dispersion quality. The results are discussed in detail in the following sections.

### 3.2. Mechanical Properties of h-BN-Reinforced PP Composites.

The mechanical properties of h-BN-reinforced PP composites, including tensile strength (TS), elongation at break (*E*%), and toughness, are summarized in Table 2, while the stress–strain curves for these samples are shown in Figure 4.

Neat HP exhibited superior tensile strength (30.42 ± 1.5 MPa) compared to impact copolymer PP (IP), attributed to its higher crystallinity. However, HP showed lower elongation and toughness, highlighting its stiffness but reduced ductility. The addition of stacked h-BN (hBN-HP) led to a reduction in both tensile strength and toughness, primarily due to the agglomeration of h-BN particles, which act as stress concentrators and hinder stress transfer.[33] Conversely, the

### Table 2. Tensile Data of PP and h-BN Reinforced PP Samples

| samples | tensile strength (TS, MPa) | elongation (*E*, %) | toughness (MPa) |
|---|---|---|---|
| HP | 30.42 ± 1.5[a] | 20.13 ± 3 | 10.51 ± 2.8 |
| hBN-HP | 29.7 ± 1.47 | 22.26 ± 9.5 | 6.81 ± 3.5 |
| e-hBN-HP | 32.88 ±. 45 | 24.86 ± 4 | 11.73 ± 1 |
| IP | 17 ± 1.8 | 369.9 ± 123 | 76 ± 30.1 |
| hBN-IP | 18.3 ± 1 | 46.26 ± 18.7 | 11.4 ± 2.6 |
| e-hBN-IP | 19.6 ± 0.9 | 333.94 ± 20.3 | 48.52 ± 17.6 |

[a] Standard error of the mean values.

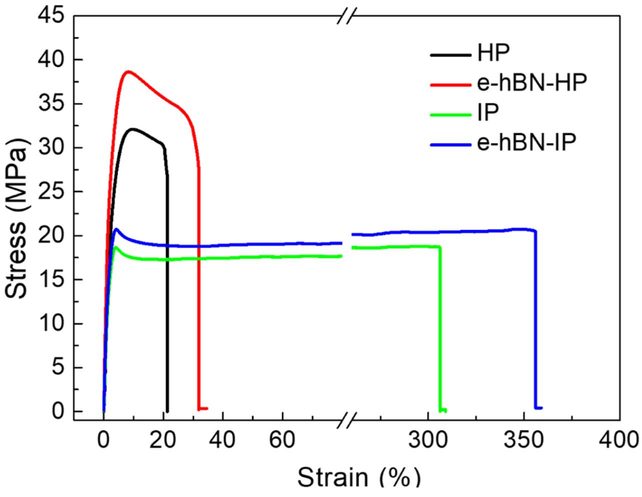

**Figure 4.** Stress−strain curves for PP and h-BN-reinforced PP samples.

incorporation of exfoliated h-BN (e-hBN-HP) significantly improved tensile strength (32.88 ± 0.45 MPa, a 14.3% increase; $p = 0.03$) and toughness (11.73 ± 1 MPa, an 11.6% increase; $p = 0.07$). These enhancements are attributed to the uniform dispersion of e-hBN nanosheets within the polymer matrix, enabling efficient stress transfer, as confirmed by XRM imaging (Figure S1).

In comparison, IP samples displayed higher elongation and toughness compared to HP, due to the rubbery ethylene domains in the matrix. However, the incorporation of stacked h-BN (hBN-IP) significantly decreased both elongation and toughness, likely caused by poor filler dispersion and weak filler−matrix interfacial interactions. The incorporation of exfoliated h-BN (e-hBN-IP) also led to a reduction in elongation and toughness for IP samples, although the decrease was less pronounced compared to stacked h-BN. These observations suggest that the limited improvement in mechanical properties of e-hBN-IP composites arises from suboptimal interfacial interactions between the IP matrix and the h-BN nanosheets, as well as the intrinsic heterogeneity of the IP matrix. This trend is consistent with findings reported by Chan et al., who observed negligible changes in mechanical properties with the addition of 10%, 15%, and 20% h-BN.[34] Thus, the mechanical properties of PP composites can be significantly improved by incorporating exfoliated h-BN nanosheets, particularly in homopolymer PP. The observed enhancement in tensile strength and toughness is attributed to the uniform dispersion and effective stress transfer enabled by the exfoliated h-BN. Optimizing dispersion techniques and enhancing filler−matrix interactions could further improve the mechanical properties of these composites, especially in matrices with more complex structures like impact copolymer PP. The mechanical properties of the composites developed in this study were compared with literature reports on h-BN-

### Table 3. Comparison of Properties of HBN Reinforced Polypropylene Composites (Published Reports) with the Presented Work

| no. | h-BN reinforced PP samples | tensile strength (MPa) | elongation (%) | OIT (mins) | $T_m$, $T_d$ (°C) | thermal conductivity (W/mK) | refs |
|---|---|---|---|---|---|---|---|
| 1 | HP | 30.42 | 20.1 | 4.6 | 163, 450 | 0.3 | this work |
| | 5%hBN-HP | 32.88 | 24.86 | 9.6 | 163, 440 | 0.7 | |
| | IP | 17 | 369.9 | 11 | 163, 475 | | |
| | 5%hBN-IP | 19.6 | 334 | 34 | 163, 475 | | |
| 2 | PP | 25.86 | 362.6 | 8.84 | 166.9, 452 | | 35 |
| | 3%hBN-PP composite | 39.49 | 7.78 | 17.82 | 165.6, 458 | | |
| 3 | PP | 31 | 248 | | 165 | 0.23 | 36 |
| | PP-hBN nanosheets | 29.1 | 35.6 | | 164 | 0.30 | |
| | PP-Alkyl grafted boron nitrides sheets | 33.4 | 120 | | 165 | 0.34 | |
| 4 | PP | 28.6 (flexural) | 2.1 (flexural E%) | | | 0.26 | 37 |
| | PP+30%hBN | 50.5 | 3.5 | | | 0.62 | |
| 5 | PP | 26.2 | >600 | | | | 38 |
| | PP+4.5% hBN | 26.5 | >600 | | | | |
| 6 | PP | 36 | 40 | | 166, 451 | | 39 |
| | 1 wt % hBN PP | 37.5 | 30 | | 169, 456 | | |
| 7 | PP | 42 | 24 | | 140 | <0.5 | 40 |
| | 5%BNI | 37 | 23 | | 145 | <0.5 | |
| | 5%BNII | 38 | 21 | | 145 | <0.5 | |
| 8 | PP | | | | 100 | <0.5 | 41 |
| | 15 Vol % | | | | 115 | 0.6 | |
| 9 | PP | 12 | 4% | | | 0.3 | 42 |
| | 5 wt % in plane | 21 | 15 | | | 0.4 | |
| | 5 wt % out plane | | | | | 0.3 | |

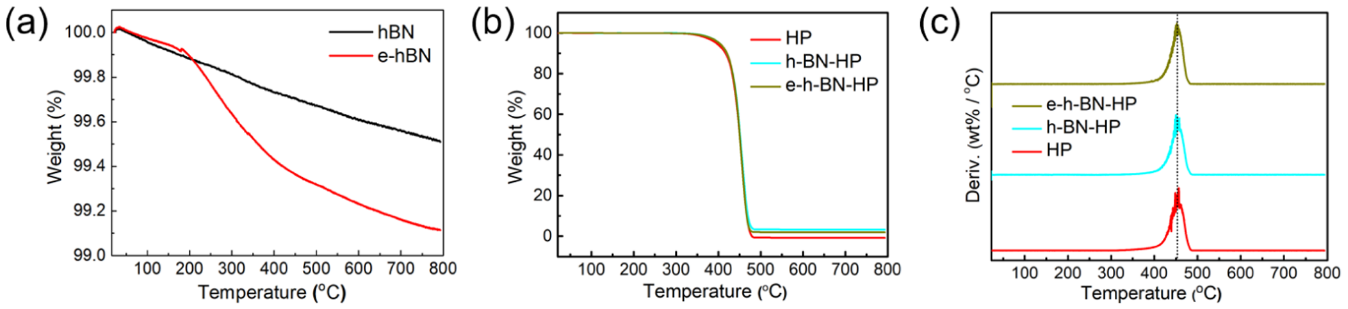

**Figure 5.** (a) TGA curves of h-BN and e-hBN, (b) TGA curves of neat HP, h-BN-HP, and e-hBN-HP samples, (c) DTGA curves of neat HP, h-BN-HP, and e-hBN-HP samples.

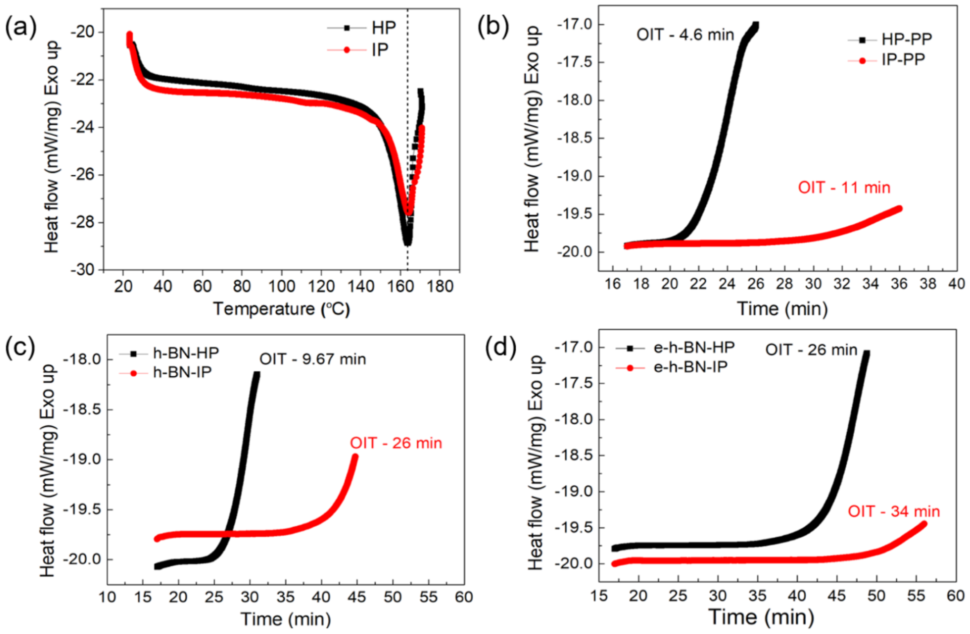

**Figure 6.** (a) DSC curves showing the melting peaks of HP and IP PP samples, and OIT measurement at 180 °C for (b) the neat HP and IP samples, (c) hBN-HP and hBN-IP composite samples, (d) e-hBN-HP and e-hBN-IP composite samples.

reinforced PP composites (Table 3). The tensile strength and toughness achieved in e-hBN-reinforced HP composites (e-hBN-HP) are competitive, demonstrating the effectiveness of exfoliated h-BN in enhancing composite performance.

### 3.3. Thermal Properties of h-BN-Reinforced PP Composites.

Thermogravimetric analysis (TGA) and derivative thermogravimetric analysis (DTGA) were used to investigate the thermal stability of polypropylene (PP) composites reinforced with h-BN. Figure 5a shows the TGA curves for h-BN and exfoliated h-BN (e-hBN), demonstrating that h-BN itself has excellent thermal stability with less than 1% weight loss.

The e-hBN sample exhibits a small weight loss, attributed to the residual poly(4-vinylpyridine) (P4VP), used as a dispersing agent during the preparation of e-hBN. However, despite h-BN's high thermal stability, there was no significant improvement in the thermal decomposition of PP with the addition of h-BN, as shown in Figure 5b,c. The decomposition temperatures of neat HP, h-BN-HP, and e-hBN-HP samples were approximately 450 °C, with similar degradation rates. A similar trend is observed for h-BN-IP samples, and thus TGA and DTGA data for these samples are provided in Figure S2. This indicates that the addition of h-BN does not significantly alter the thermal decomposition behavior of the PP matrix, although the presence of h-BN contributes to maintaining the structural integrity of the composite at higher temperatures.

DSC measurements were performed to analyze the crystallinity and melting characteristics of the PP composites. The crystallinity percentage was calculated using the formula: crystallinity (%) $= \frac{\Delta H_f}{\Delta H_f^\circ}$ where $\Delta H_f$ is the heat of fusion for the PP samples, and $\Delta H_f^\circ$ is the heat of fusion for pure crystalline PP (207 J/g).[29] The crystallinity percentages for neat HP and IP were found to be 35.3 and 31.5%, respectively, with the melting peak for both samples observed at 163 °C (Figure 6a). The difference in crystallinity between HP and IP correlates with their mechanical properties, where HP, with its higher crystallinity, shows increased strength, while the lower crystallinity of IP contributes to its enhanced ductility. Despite the addition of h-BN to PP composites, no significant improvement in the thermal properties of PP was observed, indicating that h-BN reinforcement does not notably affect the crystallinity or melting characteristics of the polymer matrix, as shown in Table 3.

Oxygen induction time (OIT) was measured to evaluate the oxidative thermal stability of the PP composites (Figure S3). The OIT values were determined at 180 °C, as OIT values at 200 and 220 °C were impractical due to values being less than

1 min. For neat HP and IP, the OIT values were 4.6 and 11 min, respectively (Figure 6b). The addition of h-BN increased OIT to 9.67 min for h-BN-HP and 26 min for h-BN-IP (Figure 6c). Further enhancement was observed with exfoliated h-BN, leading to OIT values of 13 min for e-hBN-HP and 34 min for e-hBN-IP (Figure 6d). These results indicate that the addition of hexagonal boron nitride (h-BN), particularly in its exfoliated form (e-hBN), significantly improves the oxidative stability and thermal performance of polypropylene (PP) composites. The increase in oxidative induction time (OIT) observed in the h-BN and e-hBN-reinforced PP samples suggests that h-BN acts as an effective barrier to oxygen diffusion, thus delaying the onset of oxidation. The better dispersion of e-hBN within the PP matrix further enhances this protective effect, as evidenced by the higher OIT values for the e-hBN-HP and e-hBN-IP samples compared to their nonexfoliated counterparts. This improved oxidative stability is partly attributed to the high thermal conductivity of h-BN, which enhances the heat dissipation properties of the composite. In addition to the OIT measurements, thermal conductivity measurements also provide important insights into the composite's thermal performance. The addition of thermally conductive h-BN improves the thermal conductivity of the PP matrix, contributing to better heat dissipation. The e-hBN-reinforced composites show even higher thermal conductivity (Figure 7), likely due to the superior dispersion of e-hBN in the PP matrix, enhancing the heat dissipation properties of the composite.

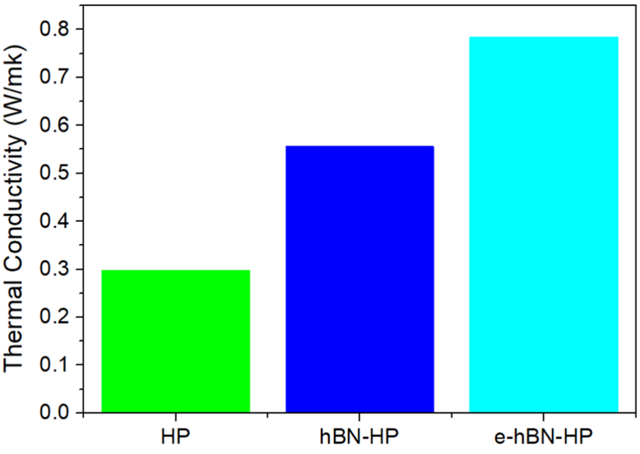

**Figure 7.** Thermal conductivity of neat HP, hBN-HP and e-hBN-HP.

The oxidation resistance of the composites was evaluated through thermal aging studies, where both HP and IP samples were subjected to 120 °C for 250 and 500 h to simulate long-term thermal exposure. To monitor the formation of oxidized products, particularly the carbonyl (−C═O) group, Fourier-transform infrared (FTIR) spectroscopy was employed.

The FTIR spectra (Figure 8a) showed the characteristic absorption peaks of the carbonyl group in the 1700−1780 cm$^{-1}$ region, which is indicative of polymer oxidation.[12] The carbonyl index (CI) is an effective measure for assessing the extent of oxidation in polymer samples, calculated as the ratio of the intensity of the carbonyl peak (1700−1780 cm$^{-1}$) to the reference peak (2730 cm$^{-1}$). As expected, thermal aging of the neat HP and IP samples led to a significant increase in the intensity of the carbonyl peaks, with the carbonyl index (CI) showing a noticeable rise. For HP samples, the CI values increased from 0.12 (neat) to 1.14 after 250 h and to 1.17 after 500 h of aging, signaling substantial oxidation. Similarly, for IP samples, the CI values increased from 0.18 (neat) to 1.0 after 250 h and 1.25 after 500 h, suggesting considerable oxidation over time. However, the addition of h-BN nanosheets to the PP matrix significantly improved the oxidation resistance, as indicated by lower CI values for both h-BN and exfoliated h-BN (e-hBN) reinforced HP and IP samples compared to their thermally aged counterparts without h-BN. The FTIR results further support the findings from the OIT studies, confirming that the addition of h-BN nanosheets, both nonexfoliated and exfoliated, enhanced the oxidation resistance of the PP composites. The h-BN-reinforced samples exhibited lower CI values compared to the thermally aged PP samples without h-BN, indicating a reduction in the extent of oxidation. This suggests that the incorporation of h-BN nanosheets, especially exfoliated ones, improves the material's resistance to oxidation under thermal aging conditions.

## 4. CONCLUSIONS

In conclusion, this study demonstrates that the incorporation of exfoliated hexagonal boron nitride (h-BN) nanosheets significantly enhances the thermal and mechanical properties of polypropylene (PP) composites. The exfoliation process of h-BN was key to achieving a more uniform dispersion of nanosheets within the PP matrix, which in turn led to improved mechanical and thermal properties. h-BN powders were exfoliated using a high-pressure homogenizer in a liquid phase, effectively separating the h-BN layers into nanosheets and ensuring their uniform distribution within the PP matrix. TGA and DTGA analyses revealed that the addition of h-BN

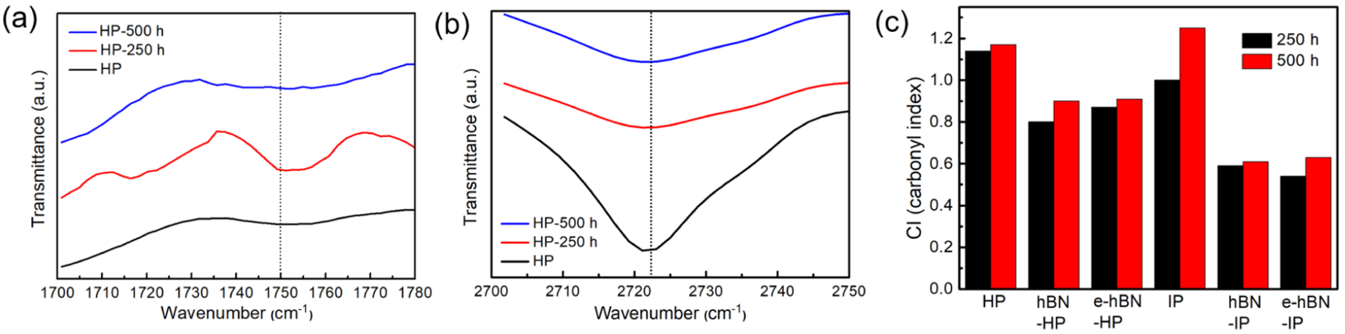

**Figure 8.** FTIR spectra of the neat and aged HP samples showing (a) the carbonyl peak in the 1700−1780 cm$^{-1}$ region and (b) − CH stretching reference peak in the 2700−2750 cm$^{-1}$ range. (c) carbonyl index (CI) values for thermally aged PP and h-BN-reinforced PP samples.

https://doi.org/10.1021/acsomega.4c10677
*ACS Omega* 2025, 10, 1853−1861

did not significantly alter the thermal decomposition temperatures. However, DSC and OIT measurements indicated an increase in oxidative thermal stability, particularly with exfoliated h-BN. The exfoliated h-BN also enhanced the oxidative induction time (OIT) and reduced the carbonyl index values in thermally aged samples, demonstrating improved oxidation resistance. FTIR analysis further confirmed this enhanced oxidation resistance, with lower carbonyl index values observed in the h-BN-reinforced samples. Additionally, the inclusion of h-BN, especially exfoliated h-BN, improved the thermal conductivity of the PP matrix, suggesting its potential for applications requiring efficient thermal management. Overall, these findings highlight the importance of filler dispersion and matrix compatibility in optimizing the performance of h-BN-PP composites. The exfoliated h-BN not only provided enhanced mechanical reinforcement but also significantly improved the thermal stability and oxidation resistance of the composites, making them promising candidates for various industrial applications.

## ■ ASSOCIATED CONTENT

### Supporting Information

The Supporting Information is available free of charge at https://pubs.acs.org/doi/10.1021/acsomega.4c10677.

> Additional detailed figures, and tables about materials characterization and mechanical and thermal testing results (PDF)

## ■ AUTHOR INFORMATION

### Corresponding Authors

**Tae Hee Lee** − *Premium Vehicle R&D Center, Jeonnam Division, Korea Automotive Technology Institute, Yeongam-gun, Jeollanam-do 58463, South Korea*; Email: thlee@katech.re.kr

**TaeYoung Kim** − *Department of Materials Science and Engineering, Gachon University, Seongnam-si, Gyeonggi-do 13120, South Korea; R&D Center, ENCAT, #1001 SICOX Tower, Seongnam-si, Gyeonggi-do 13229, Republic of Korea;* orcid.org/0000-0001-8156-4438; Email: taeykim@gachon.ac.kr

### Authors

**Amit Kumar Sonker** − *Department of Materials Science and Engineering, Gachon University, Seongnam-si, Gyeonggi-do 13120, South Korea; BA5409 Cellulose Films and Coatings, BA54 Biomaterials Processing and Products, VTT Technical Research Center of Finland, Espoo 02150, Finland;* orcid.org/0000-0003-3825-632X

**Man Hieu Tran** − *Department of Materials Science and Engineering, Gachon University, Seongnam-si, Gyeonggi-do 13120, South Korea*

**Nathan Park** − *Department of Physics, University of California, Santa Barbara, California 93106, United States*

**Gouri Sankar Das** − *Department of Materials Science and Engineering, Gachon University, Seongnam-si, Gyeonggi-do 13120, South Korea*

**Hansa Mahajan** − *Department of Materials Science and Engineering, Gachon University, Seongnam-si, Gyeonggi-do 13120, South Korea;* orcid.org/0000-0003-1393-4518

Complete contact information is available at: https://pubs.acs.org/10.1021/acsomega.4c10677

### Author Contributions

#A.K.S. and M.H.T. contributed equally to this work.

### Notes

The authors declare no competing financial interest.

## ■ ACKNOWLEDGMENTS

This work was supported by the Gachon University research fund of 2019 (GCU-2019-0832). This work was supported by the Gachon University research fund of 2022 (GCU-202208920001). This work was supported by Korea Institute for Advancement of Technology (KIAT) grant funded by the Korea Government (MOTIE) (P0007281, Development eco-friendly foam-free steering wheel for commercial and SUVs).

## ■ REFERENCES

(1) Maier, C.; Calafut, T. Applications; Maier, C.; Calafut, T., Eds.; Polypropylene, William Andrew Publishing: Norwich, NY, 1998; Chapter 11, pp 87−107.

(2) Jayaraman, K.; Kumar, S. Polypropylene Layered Silicate Nanocomposites; Mai, Y.-W.; Yu, Z.-Z., Eds.; Woodhead Publishing, 2006; Chapter 4, pp 130−150.

(3) Manias, E.; Touny, A.; Wu, L.; Strawhecker, K.; Lu, B.; Chung, T. C. Polypropylene/Montmorillonite Nanocomposites. Review of the Synthetic Routes and Materials Properties. *Chem. Mater.* **2001**, *13* (10), 3516−3523.

(4) Arjmandi, R.; Hassan, A.; Othman, N.; Mohamad, Z. Characterizations of Carbon-Based Polypropylene Nanocomposites. In *Carbon-Based Polymer Nanocomposites for Environmental and Energy Applications*; Ismail, A. F.; Goh, P. S., Eds.; Elsevier, 2018; Chapter 3, pp 57−78.

(5) Mittal, G.; Dhand, V.; Rhee, K. Y.; Park, S.-J.; Lee, W. R. A review on carbon nanotubes and graphene as fillers in reinforced polymer nanocomposites. *J. Ind. Eng. Chem.* **2015**, *21*, 11−25.

(6) Balandin, A. A.; Ghosh, S.; Bao, W.; Calizo, I.; Teweldebrhan, D.; Miao, F.; Lau, C. N. Superior Thermal Conductivity of Single-Layer Graphene. *Nano Lett.* **2008**, *8* (3), 902−907.

(7) Lee, C.; Wei, X.; Kysar, J. W.; Hone, J. Measurement of the Elastic Properties and Intrinsic Strength of Monolayer Graphene. *Science* **2008**, *321* (5887), 385−388.

(8) Stoller, M. D.; Park, S.; Zhu, Y.; An, J.; Ruoff, R. S. Graphene-Based Ultracapacitors. *Nano Lett.* **2008**, *8* (10), 3498−3502.

(9) Treacy, M. M. J.; Ebbesen, T. W.; Gibson, J. M. Exceptionally high Young's modulus observed for individual carbon nanotubes. *Nature* **1996**, *381* (6584), 678−680.

(10) Ebbesen, T. W.; Lezec, H. J.; Hiura, H.; Bennett, J. W.; Ghaemi, H. F.; Thio, T. Electrical conductivity of individual carbon nanotubes. *Nature* **1996**, *382* (6586), 54−56.

(11) Hegde, R. R.; Bhat, G. S.; Spruiell, J. E.; Benson, R. Structure and properties of polypropylene-nanoclay composites. *J. Polym. Res.* **2013**, *20* (12), 323.

(12) Ramos Filho, F. G.; Mélo, T. J. A.; Rabello, M. S.; Silva, S. M. L. Thermal stability of nanocomposites based on polypropylene and bentonite. *Polym. Degrad. Stab.* **2005**, *89* (3), 383−392.

(13) Inuwa, I. M.; Che Abdul Razak, N.; Arjmandi, R.; Hassan, A. Effects of halloysite nanotubes on the mechanical, thermal, and flammability properties of PP-g-MAH compatibilized polyethylene terephthalate/polypropylene nanocomposites. *Polym. Compos.* **2018**, *39* (S3), E1554−E1564.

(14) Song, K.; Zhang, Y.; Meng, J.; Green, E. C.; Tajaddod, N.; Li, H.; Minus, M. L. Structural Polymer-Based Carbon Nanotube Composite Fibers: Understanding the Processing−Structure−Performance Relationship. *Materials* **2013**, *6* (6), 2543−2577.

(15) Ma, P.-C.; Siddiqui, N. A.; Marom, G.; Kim, J.-K. Dispersion and functionalization of carbon nanotubes for polymer-based nanocomposites: A review. *Compos. A: Appl. Sci. Manufact.* **2010**, *41* (10), 1345−1367.

(16) Li, Y.; Yang, M.; Xu, B.; Sun, Q.; Zhang, W.; Zhang, Y.; Meng, F. Synthesis, structure and antioxidant performance of boron nitride (hexagonal) layers coating on carbon nanotubes (multi-walled). *Appl. Surf. Sci.* **2018**, *450*, 284−291.

(17) Haubner, R.; Wilhelm, M.; Weissenbacher, R.; Lux, B. Boron Nitrides — Properties, Synthesis and Applications. In *High Performance Non-Oxide Ceramics II*; Jansen, M., Ed.; Springer Berlin Heidelberg: Berlin, Heidelberg, 2002; pp 1−45.

(18) TabkhPaz, M.; Shajari, S.; Mahmoodi, M.; Park, D.-Y.; Suresh, H.; Park, S. S. Thermal conductivity of carbon nanotube and hexagonal boron nitride polymer composites. *Composites, B* **2016**, *100*, 19−30.

(19) Shi, Y.; Hamsen, C.; Jia, X.; Kim, K. K.; Reina, A.; Hofmann, M.; Hsu, A. L.; Zhang, K.; Li, H.; Juang, Z.-Y.; Dresselhaus, M. S.; Li, L.-J.; Kong, J. Synthesis of Few-Layer Hexagonal Boron Nitride Thin Film by Chemical Vapor Deposition. *Nano Lett.* **2010**, *10* (10), 4134−4139.

(20) Song, L.; Ci, L.; Lu, H.; Sorokin, P. B.; Jin, C.; Ni, J.; Kvashnin, A. G.; Kvashnin, D. G.; Lou, J.; Yakobson, B. I.; Ajayan, P. M. Large Scale Growth and Characterization of Atomic Hexagonal Boron Nitride Layers. *Nano Lett.* **2010**, *10* (8), 3209−3215.

(21) Yu, C.; Zhang, J.; Tian, W.; Fan, X.; Yao, Y. Polymer composites based on hexagonal boron nitride and their application in thermally conductive composites. *RSC Adv.* **2018**, *8* (39), 21948−21967.

(22) Boldrin, L.; Scarpa, F.; Chowdhury, R.; Adhikari, S. Effective mechanical properties of hexagonal boron nitride nanosheets. *Nanotechnology* **2011**, *22* (50), No. 505702.

(23) Lin, Z.; Liu, Y.; Raghavan, S.; Moon, K.-s.; Sitaraman, S. K.; Wong, C.-p. Magnetic Alignment of Hexagonal Boron Nitride Platelets in Polymer Matrix: Toward High Performance Anisotropic Polymer Composites for Electronic Encapsulation. *ACS Appl. Mater. Interfaces* **2013**, *5* (15), 7633−7640.

(24) Bhimanapati, G. R.; Glavin, N. R.; Robinson, J. A. 2D Boron Nitride: Synthesis and Applications. In *Semiconductors and Semimetals*; Iacopi, F.; Boeckl, J. J.; Jagadish, C., Eds.; Elsevier, 2016; Chapter 3, pp 101−147.

(25) Yung, K. C.; Liem, H. Enhanced thermal conductivity of boron nitride epoxy-matrix composite through multi-modal particle size mixing. *J. Appl. Polym. Sci.* **2007**, *106* (6), 3587−3591.

(26) Huang, X.; Wang, S.; Zhu, M.; Yang, K.; Jiang, P.; Bando, Y.; Golberg, D.; Zhi, C. Thermally conductive, electrically insulating and melt-processable polystyrene/boron nitride nanocomposites prepared by in situ reversible addition fragmentation chain transfer polymerization. *Nanotechnology* **2015**, *26* (1), No. 015705.

(27) Joshi, M. D.; Goyal, A.; Patil, S. M.; Goyal, R. K. Tribological and thermal properties of hexagonal boron nitride filled high-performance polymer nanocomposites *J. Appl. Polym. Sci.* 2017; Vol. *134* 4, DOI: 10.1002/app.44409.

(28) Ye, D.; Li, S.; Lu, X.; Zhang, X.; Rojas, O. J. Antioxidant and Thermal Stabilization of Polypropylene by Addition of Butylated Lignin at Low Loadings. *ACS Sustainable Chem. Eng.* **2016**, *4* (10), 5248−5257.

(29) Ahmed, A. K.; Atiqullah, M.; Pradhan, D. R.; Al-Harthi, M. A. Crystallization and melting behavior of i-PP: a perspective from Flory's thermodynamic equilibrium theory and DSC experiment. *RSC Adv.* **2017**, *7* (67), 42491−42504.

(30) Zhang, B.; Wu, Q.; Yu, H.; Bulin, C.; Sun, H.; Li, R.; Ge, X.; Xing, R. High-Efficient Liquid Exfoliation of Boron Nitride Nanosheets Using Aqueous Solution of Alkanolamine. *Nanoscale Res. Lett.* **2017**, *12* (1), 596.

(31) Cao, L.; Emami, S.; Lafdi, K. Large-scale exfoliation of hexagonal boron nitride nanosheets in liquid phase. *Materials Express* **2014**, *4* (2), 165−171.

(32) Xue, Y.; Liu, Q.; He, G.; Xu, K.; Jiang, L.; Hu, X.; Hu, J. Excellent electrical conductivity of the exfoliated and fluorinated hexagonal boron nitride nanosheets. *Nanoscale Res. Lett.* **2013**, *8* (1), 49.

(33) Paiva, M. C.; Zhou, B.; Fernando, K. A. S.; Lin, Y.; Kennedy, J. M.; Sun, Y. P. Mechanical and morphological characterization of polymer−carbon nanocomposites from functionalized carbon nanotubes. *Carbon* **2004**, *42* (14), 2849−2854.

(34) Chan, K. W.; Wong, H. M.; Yeung, K. W. K.; Tjong, S. C. Polypropylene Biocomposites with Boron Nitride and Nanohydroxyapatite Reinforcements. *Materials* **2015**, *8* (3), 992−1008.

(35) Bayramoğlu, G.; Mudu, M. Processing and Characterization of Polypropylene Nanocomposite Films Reinforced with Hexagonal Boron Nitride Nanosheets. *Period. Polytech., Chem. Eng.* **2023**, *67* (1), 94−103.

(36) Kong, S.; Seo, H.; Shin, H.; Baik, J.-H.; Oh, J.; Kim, Y.-O.; Lee, J.-C. Improvement in mechanical and thermal properties of polypropylene nanocomposites using an extremely small amount of alkyl chain-grafted hexagonal boron nitride nanosheets. *Polymer* **2019**, *180*, No. 121714.

(37) Muratov, D. S.; Vanyushin, V.; Koshlakova, V. A.; Kolesnikov, E. A.; Maksimkin, A. V.; Stepashkin, A. A.; Kuznetsov, D. V. Improved mechanical and thermal properties of polypropylene filled with reduced graphene oxide (rGO) and hexagonal boron nitride (hBN) particles. *J. Alloys Compd.* **2024**, *972*, No. 172882.

(38) Chan, K. W.; Wong, H. M.; Yeung, K. W. K.; Tjong, S. C. Polypropylene Biocomposites with Boron Nitride and Nanohydroxyapatite Reinforcements. *Materials* **2015**, *8* (3), 992−1008.

(39) Divya Aparna, N.; Tambe, P. Functionalized boron nitride nanosheets and their polypropylene nanocomposites: influence on thermal, mechanical, rheological and wear behaviour. *Compos. Interfaces* **2024**, *31*, 1−28.

(40) Chen, H.; Wang, Y.; Nan, Y.; Wang, X.; Yue, X.; Zhang, Y.; Fan, H. Effects of BN on the Mechanical and Thermal Properties of PP/BN Composites. *J. Wuhan Univ. Technol.-Mater. Sci. Ed.* **2024**, *39* (2), 345−352.

(41) Cheewawuttipong, W.; Fuoka, D.; Tanoue, S.; Uematsu, H.; Iemoto, Y. Thermal and Mechanical Properties of Polypropylene/Boron Nitride Composites. *Energy Procedia* **2013**, *34*, 808−817.

(42) Liu, X.-X.; Huang, Y.-Z.; Huang, Z.-X. Compatibilizing and functionalizing polypropylene/polyethylene by in-situ exfoliating hexagonal boron nitride at interface. *Compos. Sci. Technol.* **2022**, *221*, No. 109354.